A Moving Mesh Approach to a Shallow Ice

Abstract

is described in detail in Section 3 below. There are two boundary conditions: a no-flux condition at the ice divide (at $x = 0$) and zero ice thickness at the moving front, i.e.

$$\frac{\partial h}{\partial x} = 0 \quad \text{at } x = 0; \qquad h = 0 \quad \text{at } x = b(t): \tag{2}$$

The total ice in the whole domain, denoted here by (t), is defined as

$$\int_0^{b(t)} h(x;t)\,dx = \ (t); \tag{3}$$

and has the following property, to be referred to later. Differentiating eq. (3) with respect to t using Leibnitz' integral rule gives

$$\dot{\ } = \frac{d}{dt}\int_0^{b(t)} h(x;t)\,dx \tag{4}$$

$$= \int_0^{b(t)} \frac{\partial h}{\partial t}\,dx + h(b;t)\frac{db}{dt} \tag{5}$$

Since $h = 0$ at $x = b(t)$ the second term is zero. Substituting eq. (1) into eq. (5) results in

$$\dot{\ } = \int_0^{b(t)} \frac{\partial (hu)}{\partial x}\,dx + \int_0^{b(t)} m(x)\,dx \tag{6}$$

$$= \ hu\Big|_{x=0}^{b(t)} + \int_0^{b(t)} m(x)\,dx$$

Use of the boundary conditions, eq. (2), again forces the first term to be zero, since the ice flow is zero at the ice divide. This leaves the rate of change of the total ice over the domain as

$$\dot{\ } = \int_0^{b(t)} m(x)\,dx: \tag{7}$$

As a result any change in the total ice over the whole glacier is due solely to the source term in eq. (7), i.e. the rate of change of global ice thickness equates to the net accumulation/ablation over the whole glacier.

3 Diffusive Velocity at the Glacier Front

The diffusive flow velocity of glaciers ($u(x;t)$ in eq. (1)) is typically dominated movement of the glacier front generated by this diffusive flow velocity is assessed.

Under the shallow ice approximation the diffusive velocity $u(x;t)$ in eq. (1) can be written as

$$u(x;t) = c\{h(x;t)\}^{n+1} s_x^n; \tag{8}$$

(see e.g. [9]) under the assumption that temperature and density remain constant throughout the glacier, where c is a negative constant. The surface elevation s(x) is the glacier height comprising the topographical bed and where the function $g(x;t) > 0$ is nite and has a nite x derivative atax

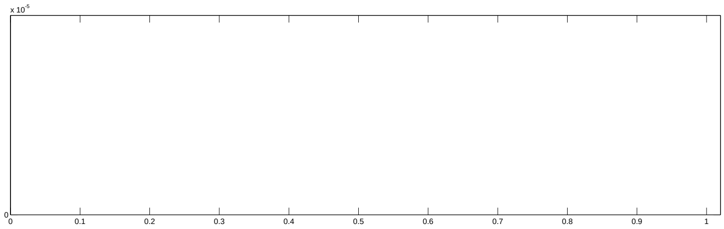

x 10^-6
0
0
0.1
0.2
0.3
0.4
0.5
0.6
0.7
0.8
0.9
1

3.2 Introducing topography

Removing the assumption that the bed of the glacier is at, the surface elevation is a summation of the bed and ice components

$$s(x; t) = z(x) + h(x; t); \tag{19}$$

where $z(x)$ represents the topography under the glacier. With $n = 3$ the di usive velocity in eq. (8) may then be written as

$$u(x; t) = c f h(x; t) g^4 (f z(x) + h(x; t) g_x)^3 \tag{20}$$

$$= c z_x^3 f h(x; t) g^4 + 3 c z_x^2 f h(x; t) g^4 h_x + 3 c z_x f h(x; t) g^4 h_x^2 + c f h(x; t) g^4 h_x^3 : \tag{21}$$

The last term in eq. (21) is the same as the single term in the at bed scenario, eq. (9) with $n = 3$. Expressing the terms in eq. (21) in the form used in eq. (10) gives

$$u(x; t) = c(z_x) f h(x; t) g^4 + \frac{3c}{5}(z_x)^2 \quad f h(x; t) g^5 \;_x + \frac{c}{3} z_x \quad f h(x; t) g^3 \;_x \;^2 + \frac{9c}{343} \; n \quad f h(x; t) g^{7=3} \;_x \; o_3 : \tag{22}$$

Substituting for h from eq. (11),

$$u(x; t) = c(z_x)^3 (b \quad x)^4 \; f g(x; t) g^4 + \frac{3c}{5}(z_x)^2 \quad (b \quad x)^5 \; f g(x; t) g^5 \;_x + \frac{c}{3} z_x \quad (b \quad x)^3 \; f g(x; t) g^3 \;_x \;^2 + \frac{9c}{343} \; n \; (b \quad x)^{7 = 3} f g(x) g^{7=3} \;_x \; o \;^3 : \tag{23}$$

At the moving boundary the di usive v

the remaining three terms individually, leaves

$$
\begin{aligned}
u(b;t) = & -\frac{3c}{5}(z_b)^2 \lim_{x\to b} (b-x)^{5\beta-1}\{g(x)\}^5 \\
& + \frac{c}{3} z_b \left[\lim_{x\to b} \{(b-x)^{3\beta-1}\}\{g(x;t)\}^3 \right]^2 \\
& + \frac{9c}{343} \left[\lim_{x\to b} \{(b-x)^{7\beta/3-1}\}\{g(x;t)\}^{7/3} \right]^3 . \quad (25)
\end{aligned}
$$

Each term separately yields a different critical value of β, namely $\beta_c = 1/5; 1/3$ and $3/7$ for each term respectively. However, since β cannot go below any of these values without encountering an infinite velocity (see section 3.1), the lower limit for

Since $h \to 0$ the limit in eq. (31) as $b \to b$

Physical Parameters	
$n = 3$	Flow-law exponent
$A = 10\ ^{16}(Pa)\ ^{3}a\ ^{1}$	Flow-law parameter
$g = 9{:}81ms\ ^{2}$	Acceleration of gravity
$= 910kgm\ ^{3}$	Ice density
$c = \ 2Ag^{n}\ ^{n} = (n + 2)$	Constant Parameter
$= 0{:}0005$	Scale of accumulation rate

state solution is greater than the initial boundary position and the overall motion is that of an advance. Figure 2a) demonstrates an overall increase in the amount of ice in the domain, along with movement of the front towards the steady state boundary $b_{ss} = \sqrt{1.5}$. With $= 3/7$ there is an initial diffusive velocity contributing to the movement of the boundary (see fig. 3a)).

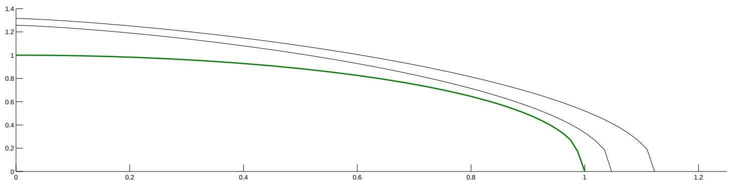

0
0.2
0.4
0.6
0.8
1
1.2
1.4

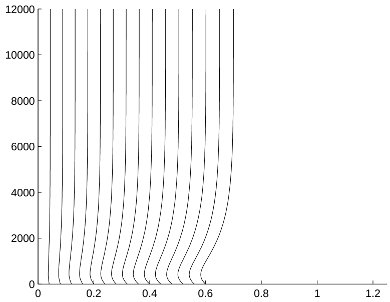
12000
10000
8000
6000
4000
2000
0
0
0.2
0.4
0.6
0.8
1
1.2

corresponding to the source term only, which is

$$m(x) = \min\{0.5;\ (\quad x)\}; \tag{47}$$

The initial profile of ice thickness is therefore

$$h^0(x) = \quad t \quad \min\{0.5;\ (\quad x)\} \tag{48}$$

with $x \in [0; 4.5 \quad 10^5$

The physical parameters are provided in table 2 along with the numerical data. For direct comparison with the results in [7] the model uses 61 grid points, initially spaced evenly. This allows for a time step of 2a, up to a final time of 30000a. The calculation takes less than five seconds to run on a standard desktop.

For such a radially symmetric problem the results of the one-dimensional flowline method may be presented as a circle which allows for ease of comparison with the two-dimensional data.

The numerical solutions to the experiment given in [7] are traditional fixed grid methods on evenly spaced grids. This means that they require some form of extrapolation or interpolation to find the boundary location as the boundary generally falls between two grid points. As a result the fixed grid methods on a regular two-dimensional rectangular grid, such as those presented, do not return a perfect circle due to the location of the grid points, as shown in fig. 4a). This is not an issue with radial flowline methods such as the one used here, which when rotated naturally give a circle (see fig. 4b)).

A better comparison is a direct comparison between flowline models. The moving mesh method is able to get significantly closer to the exact ice thickness profile than the equivalent fixed grid method in Figure 4c), especially near to the moving front. In Figure 4d) the diffusive velocity in steady state is similar in the two approaches, the main difference again arising at the boundary where the diffusive velocity can be explicitly calculated in the moving mesh approach. The fixed grid schemes require interpolation to calculate this value.

Expressing these results in table 3 shows that the CMF moving mesh solution is able to get much closer to the exact boundary position than the average fixed grid solution, whilst the thickness at the ice divide (where $x = 0$) is slightly higher than both the fixed grid and exact solutions.

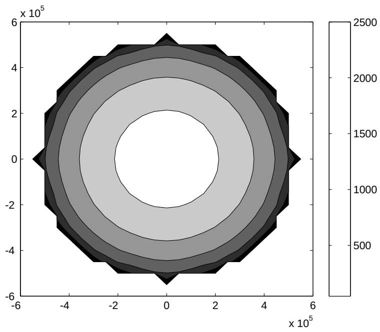
x 10^5
6
4
2
0
-2
-4
-6
-6
-4
-2
0
2
4
6
x 10^5
2500
2000
1500
1000
500

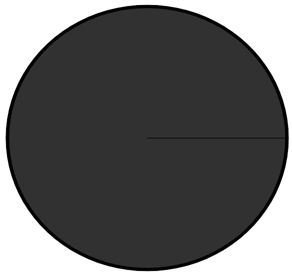

8 Data Assimilation

While numerical models of ice sheets provide a good representation of the dynamical flow, uncertainties in the initial input data lead to errors as the simulation evolves. Moreover, observations describing the glacier system are incomplete and contain inaccuracies. Using data assimilation the two can be combined to gain a best representation of the true state of the ice sheet.

Here we employ a sequential assimilation approach, where the model is evolved from a-priori initial estimates until observations are available. The model prediction of the variables, denoted z^f, is then corrected by a weighted difference between the observations y and the predicted observations Cz^f to obtain the analysis z^a, the best representation. Mathematically a

Value	Quantity
z	Vector containing the unknown model variables
y	Vector of observations
a	Superscript denoting the 'analysis', or best guess solution
f	Superscript denoting the prior solution, taken from the model
C	Observation operator mapping observations to the model space
$K = BC^T(CBC^T + R)^{-1}$	Correction, or Gain Matrix
B	Background error covariance matrix
R	Observation error covariance matrix

Table 4: Data Assimilation variables

solution are applied and an assimilation step is performed. This procedure is known as a twin experiment. The state vector represents all the unknown values of the ice thickness, $z = \{H_i\}_{i=1}^{N}$.

The observations are subject to random noise, $y = Cz^a + e$, where $e \in N(0; \sigma_o^2)$ to simulate observation errors. Each observation is assumed independent of the others, so the covariance between them is zero and $R = \sigma_o^2 I$. Since the observations are direct, linear interpolation is used to calculate the predicted observations for the matrix C. We assume that the observations of ice thickness are within $\sqrt{30}$m of the truth, i.e. $\sigma_o^2 = 30$.

The choice of the background error covariance matrix B is one of the most critical aspects of any data assimilation scheme, primarily representing the covariance relationship between the variables, although it also acts to spread information between variables. For fixed grid methods a typical correlation function between variables i and j to characterise the background errors is the

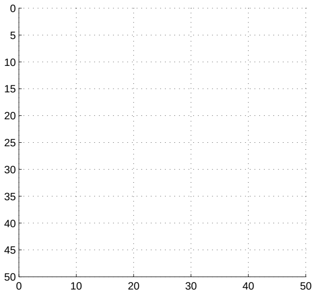

0
5
10
15
20
25
30
35
40
45
50
0
10
20
30
40
50

The ice thickness at the divide (g. 6(b)) is corrected at the time of assimilation,

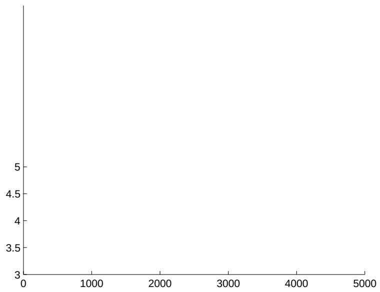

5
4.5
4
3.5
3
0
1000
2000
3000
4000
5000

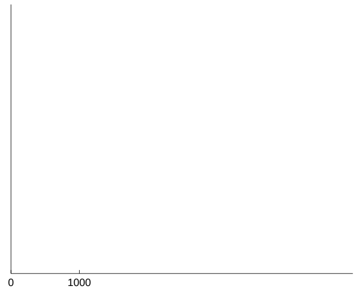
0
1000

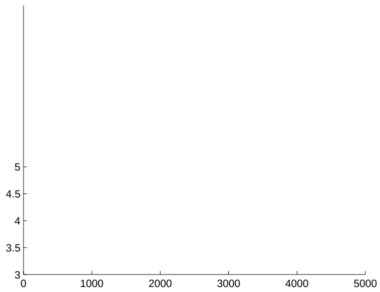
5
4.5
4
3.5
3
0
1000
2000
3000
4000
5000

noted that information is implicitly transfered through fu rther iterations which

[8] D. Partridge and M. J. Baines. A moving mesh approach to anice sheet model. Computers and Fluids, 46, 2011.